



The *Clock* mutation reduces reproductive performance of mice by affecting the implantation capacity: Maternal *Clock* mutation is not the only factor affecting implantation



Tomoko Amano^{a,b,*}, Masayuki Anzai^c, Kazuya Matsumoto^a

^aDepartment of Genetic Engineering, College of Biology-Oriented Science and Technology, Kindai University, Kinokawashi, Wakayama, Japan

^bLaboratory of Animal Genetics, Department of Sustainable Agriculture, College of Agriculture, Food and Environmental Science, Rakuno Gakuen University, Ebetsu, Hokkaido, Japan

^cInstitute of Advanced Technology of Kindai University, Kainan, Wakayama, Japan

ARTICLE INFO

Article history:

Received 5 August 2015

Received in revised form 4 May 2016

Accepted 20 May 2016

Keywords:

Circadian gene

Mouse

Implantation

ABSTRACT

Here, we showed that the *Clock* gene was important for reproductive performance in mice. We compared outcomes from the four possible mating combinations between wild-type mice (WT) and mice homozygous for the *Clock delta-19* mutation (*CL*). We found that the only significant differences were between the $WT\delta \times WT\varphi$ and $CL\delta \times CL\varphi$ mating groups; these groups differed with regard to elongation of the pregnancy period (19.3 vs. 20.5 days, respectively, $P < 0.05$) and the number of newborn pups (13.4 ± 0.8 vs. 8.6 ± 1.5 , respectively, $P < 0.05$). Because *CL* dams impregnated by male *CL*s exhibited normal continuous increases in body weight during the entire gestation period and did not show any signs of spontaneous abortion from mid to late gestation, we reasoned that some embryos were lost before or at the time of implantation. Immediately before implantation (88 hours after fertilization), neither the number of embryos collected from uteri nor the percentage of the embryos that reached the blastocyst stage differed significantly among mating groups. In contrast, immediately after implantation (160 hours after fertilization), the average number of implantation sites was significantly lower for the $CL\delta \times CL\varphi$ mating group than that for the $WT\delta \times WT\varphi$ mating group (7.0 vs. 13.0, $P < 0.05$); this decrease was accompanied by a significant lowering of the positions of implantation sites in uteri, and this lowering of the implantation sites was more severe when mothers and embryos bore more *CL* alleles ($WT\delta \times WT\varphi > CL\delta \times WT\varphi > WT\delta \times CL\varphi > CL\delta \times CL\varphi$), suggesting that the *Clock* mutation reduced the reproduction performance of the parents by affecting the implantation capacity via such as embryos' ability to implant.

© 2016 The Author(s). Published by Elsevier Inc. This is an open access article under the CC BY-NC-ND license (<http://creativecommons.org/licenses/by-nc-nd/4.0/>).

1. Introduction

Circadian genes that encode transcription factors are expressed in most organs, tissues, and cells of mammals (e.g., humans and mice) and of common domestic animals

and fowls (e.g., cows, pigs, horses, chickens, turkeys, and quails). These genes are upstream regulators of the circadian clock that regulates physiological phenomena that exhibit regular periodicity, such as sleep and wakefulness, changes in metabolic activity, and cell cycle transitions [1–3]. The circadian genes are classified into two groups: transcription-promoting factors such as *Clock* and *Arntl* and transcription-suppressing factors such as *Cry1*, *Cry2*, *Per1*, and *Per2*. CLOCK and ARNTL belong to a family of transcriptional regulators that contain bHLH and PAS

* Corresponding author. Tel.: +81 011 388 4717; fax: +81 011 387 5848.
E-mail address: amano@rakuno.ac.jp (T. Amano).

domains. CLOCK and ARNTL form a complex that binds to the E-box sequence (CACGTG) via bHLH regions to promote transcription of numerous target genes. These targets are designated Clock-controlled genes (CCGs) and have E-box sequences in their respective promoter regions. The action of CLOCK and ARNTL is rhythmically suppressed by transcription-suppressing factors, yields rhythms in the transcriptional activity of CCGs with periodicity of about 1 day, and consequently causes the rhythms in circadian physiological phenomena [4,5].

To analyze the role of CLOCK in physiological phenomena, many researchers have examined mice bearing the *Clock delta-19* mutation (hereafter designated *CL*); this mutation produces an aberrant CLOCK protein that can form heterodimers with ARNTL and bind to E-box motifs but is deficient in the ability to promote transcription of CCGs [6–9]. One study examined the reproductive performance of inbred C57/BL6 mice that bear *CL*, and in this strain, homozygous *CL* female mice that have conceptus heterozygous for *CL* show a severe reproductive phenotype; specifically, these *CL/CL* dams exhibit very poor production of newborns due to (1) reabsorption of fetuses during the mid-gestation stage (11 days after fertilization) and (2) difficulty during parturition [10]. However, experimental data derived from inbred strains (including C57/BL6) often merely represent strain-specific responses to particular experimental operations. Moreover, highly inbred strains are often not good models for animal populations with moderate or high levels of genetic variation (e.g., human and domestic animal populations) because these inbred strains are produced from continuous inbreeding for more than 20 consecutive generations, and such strains harbor very little genetic variability. Notably, mice kept in closed colonies, like ICR mice, maintain comparatively more genetic variation than do highly inbred strains, and mice from closed colonies are commonly used as models for human groups to test the safety of medicines or chemicals.

To more accurately model the influence of *CL* on reproductive performance of human or domestic animal populations, we used *CL* ICR mice instead of *CL* C57/BL6 mice for our studies. We examined the estrous cycle of female ICR mice homozygous for *CL* and the reproductive profiles of four mating groups; the reproductive profiles included measures of copulation, pregnancy, delivery, and the number of pups born. The mating groups were: male and female wild-type ICR mice ($WT\delta \times WT\varphi$), male ICR mice homozygous for *CL* and wild-type female ICR mice ($CL\delta \times WT\varphi$), wild-type male ICR mice and female ICR mice homozygous for *CL* ($WT\delta \times CL\varphi$), and male and female ICR mice homozygous for *CL* ($CL\delta \times CL\varphi$). In addition, if any abnormalities in a reproduction profile were observed for any mating group, putative causes were examined further.

2. Materials and methods

2.1. Animals

Mice homozygous for *CL* were derived from mice supplied by J. S. Takahashi (Northwestern University, Evanston, IL, USA); these original *CL* mice were originated from a

strain that comprised BALB/c and C57/BL/6J mice. A breeding colony was established by backcrossing the original *CL* mice to ICR mice (Jcl: ICR, CLEA, Tokyo, Japan), and a *CL* ICR colony was subsequently generated by interbreeding for more than 10 continuous generations using different ICR parental lines to maintain closed colony breeding [8]. After introducing *CL* ICR mice to our animal facility, we maintained the strain by introducing new JCL: ICR individuals as parents at each generation. For each experiment in this study, ICR mice homozygous for *CL* were used as *CL* mice, unless otherwise noted.

This *CL* mutation is an A-to-T transversion at the third base position of the 5' splice donor site of intron 19, and the genotype of each mouse used in this study was determined via a polymerase chain reaction assay that determines the base pair at that site [8]. Briefly, two primers were differently prepared so that one primer had an A and the other had a T at that site. Each primer was combined with the corresponding forward or reverse primer; the resulting primer sets were designated “primer set detecting wild type” or “primer set detecting *CL*.” The sequences of the forward and reverse primers in the “primer set detecting wild type” were 5'-GGTCAAGGGCTACAGGTA-3' and 5' TGGGGTAAAAAGACCTCTTGCC-3', respectively. The sequences of the forward and reverse primers in the “primer set detecting *CL*” were 5'-AGCACCTTCCTTG-CAGTTCG-3' and 5' -TGTGCTCAGACAGAATAAGTA-3', respectively. A DNA sample was extracted from each punched-out auricle tissue sample and used for two polymerase chain reaction assays, one with the “primer set detecting wild type” and the other with “primer set detecting *CL*”, to genotype each animal.

Each mouse used in this study was 8 to 12 weeks of age. Mice were kept under a cycle of 12 hours of lighting and 12 hours of darkness. The starting time of the light was counted as 0:00, and counting was continued until 24:00. All procedures involving animals conformed to the Guidelines for the Care and Use of Laboratory Animals of Kindai University and the Guidelines for the Care and Use of Laboratory Animals of Rakuno Gakuen University.

2.2. Analysis of estrous cycle progression

To assess estrous cycle progression, each female mouse was kept isolated for 22 days. During this period, vaginal smears were collected daily at 6 AM. Each smear was spread on a glass slide and stained with Giemsa solution (Invitrogen, Carlsbad, CA, USA) and then observed with a stereoscopic microscope. Smears containing nucleated and cornified cells were defined as representing the proestrous or estrous stages, respectively. The presence of leucocytes defined the metestrous-diestrous stage [11]. The estrous cycle consists of the proestrous stage, estrous stage, and metestrous-diestrous stage and progresses in order from the proestrous stage, estrous stage, to metestrous-diestrous stage. In this study, no mice showed estrous cycles that progressed in perturbed order. To compare occurrences of the estrous cycle in *WT* and *CL* mice, complete estrous cycles observed during the observation period were clarified for each animal. A complete estrous cycle was defined as an estrous cycle that had the defined beginning of the

Table 1
Profile of vaginal cytology and estrous cycle in WT and CL mice during a 22-day observation period.

WT																						
	1	2	3	4	5	6	7	8	9	10	11	12	13	14	15	16	17	18	19	20	21	22
1	c	l	l	l	n	c	c	c	c	l	l	l	n	c	c	l	l	l	l	l	l	n
2	c	c	c	l	l	l	n	c	c	l	l	n	n	c	l	l	n	c	c	c	l	n
3	l	n	c	l	l	n	c	c	c	l	l	n	c	l	l	l	n	c	c	l	l	n
4	l	l	l	n	c	l	l	l	n	c	l	l	l	n	c	l	l	l	n	c	c	l
5	c	l	l	l	n	c	l	l	l	n	c	c	l	l	l	n	c	c	c	l	l	n
6	c	c	c	l	l	l	n	c	c	l	l	n	n	c	c	l	l	n	c	c	c	l
7	l	n	c	c	c	c	l	l	l	n	c	c	l	l	l	l	n	n	c	c	c	c
8	l	l	l	n	c	c	l	l	l	n	c	c	l	l	l	l	n	c	c	c	l	n
9	n	c	c	l	n	c	c	l	l	n	c	c	l	l	l	n	c	l	l	l	n	c
10	c	l	l	l	n	c	l	l	n	c	c	l	l	n	c	l	n	c	c	l	n	c

CL																						
	1	2	3	4	5	6	7	8	9	10	11	12	13	14	15	16	17	18	19	20	21	22
1	c	l	l	n	c	c	l	l	n	c	c	l	l	n	c	c	l	l	n	c	c	l
2	l	l	l	l	n	c	c	l	l	l	n	c	c	l	l	l	n	c	c	l	l	n
3	n	c	c	c	l	n	c	c	c	l	n	n	c	c	l	n	n	c	c	l	l	l
4	n	c	c	l	l	l	n	c	c	l	l	n	c	c	l	l	l	l	n	c	c	l
5	n	c	c	l	l	l	n	c	c	l	l	n	c	c	l	l	l	l	n	c	c	l
6	c	l	l	n	c	l	l	l	n	c	l	l	n	c	c	c	c	l	l	l	n	c
7	n	n	c	c	l	l	n	c	c	l	l	n	c	c	l	l	n	c	l	l	l	l
8	c	c	c	l	l	n	c	c	c	l	l	l	n	c	c	c	l	l	l	n	c	l
9	c	c	c	l	n	c	c	l	l	n	n	c	c	l	n	c	c	l	l	n	n	c
10	n	n	c	l	l	l	n	c	l	l	n	c	c	l	l	n	c	l	l	l	n	c
11	l	n	c	c	c	c	l	l	n	c	c	l	l	n	c	c	l	l	n	c	c	l
12	l	l	n	c	c	l	l	l	n	c	l	l	l	n	c	c	l	l	n	c	c	l
13	n	c	l	l	n	c	c	l	l	n	c	l	l	n	c	c	l	n	c	c	l	n
14	l	l	l	l	n	c	l	l	n	c	c	l	l	n	c	c	l	n	c	c	l	l

WT indicates wild-type mice. CL indicates homozygous CL mice. In each table, the numbers in the left-most row are the identification numbers of the individuals used in the analysis. Each number in the top-most line indicates the day in the 22-day period. n, c, and l in the boxes indicate the days that nucleated cells, cornified cells, and leucocytes, respectively, were observed in vaginal smears. Smears containing nucleated or cornified cells were defined as representing the proestrous or estrous stage, respectively. The presence of leucocytes defined the metestrous-diestrous stage. The estrous cycle consists of the proestrous stage, estrous stage, and metestrous-diestrous stage and progresses in the order from proestrous stage, estrous stage, to metestrous-diestrous stage. A complete estrous cycle was defined as an estrous cycle that had the defined beginning of the proestrous stage and the defined end of the metestrous-diestrous stage [11]: the beginning of the proestrous stage was defined as the day that nucleated cells were observed in vaginal smears immediately after the period in which leucocytes were observed in vaginal smears, and the end of the metestrous-diestrous stage was defined as the day that leucocytes were observed in vaginal smears immediately followed by the day that nucleated cells were observed in vaginal smears. In the complete estrous cycles, the boxes containing n, c, and l are highlighted with green, blue, and yellow, respectively. The complete estrous cycles were used for the analysis for which results are shown in Figures 1 and 2.

proestrous stage and the defined end of the metestrous-diestrous stage. In the complete estrous cycle, the beginning of the proestrous stage was defined as the day that nucleated cells were observed in vaginal smears that immediately followed the period in which leucocytes were observed in vaginal smears. The end of the metestrous-diestrous stage was defined as the day that leucocytes were observed in vaginal smears that was immediately followed by the day that nucleated cells were observed in vaginal smears. The complete estrous cycles detected in the 22-day observation period are represented as the colored parts in Table 1. The number and the length of each complete estrous cycle, and the number and the length of the proestrous stage, estrous stage and metestrous-diestrous stage

in each complete estrous cycle in the observation period were also determined for each animal and used for analysis for which the results are shown in Figures 1 and 2.

2.3. Analysis of the reproduction profile

To analyze the reproductive profiles of CL mice, one male WT mouse or one male CL mouse and one female WT mouse or one female CL mouse were put into the same cage at 12 PM and were kept together continuously. For these analyses, Day 1 was defined as the second day of cohabitation. The presence or absence of vaginal plugs and the body weight of each female were recorded daily at 6 AM from Day 1. As a control, virgin WT females were kept

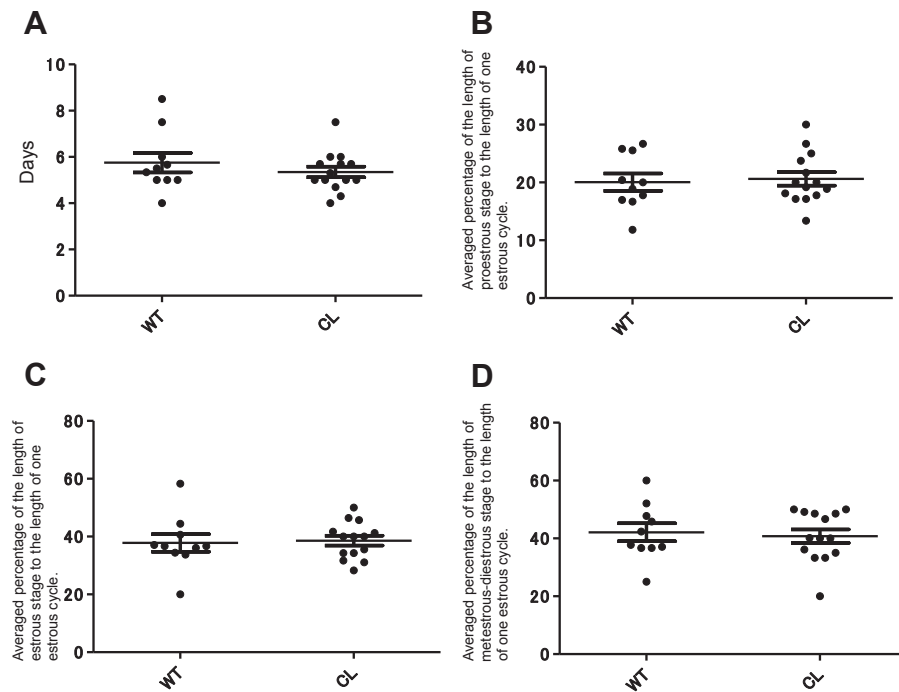


Fig. 2. Comparison of average length of one complete estrous cycle in each individual between WT female mice and homozygous *CL* female mice and comparison of averaged percentage of the lengths of proestrous, estrous, and metestrous-diestrous stages to the length of one complete estrous cycle between WT female mice and homozygous *CL* female mice. (A) Comparison of the average length of one complete estrous cycle between WT female mice and *CL* female mice. The lengths of complete estrous cycles monitored in each individual during the 22-day observation were measured and averaged. One dot corresponds to the average length of complete estrous cycles in one individual. The average length of one complete estrous cycle in each individual was calculated for WT female mice and *CL* female mice. (B) Comparison of the averaged percentage of length of the proestrous stage to the length of one estrous cycle. (C) Comparison of the averaged percentage of length of the estrous stage to the length of one estrous cycle. (D) Comparison of the averaged percentage of length of the metestrous-diestrous stage to the length of one estrous cycle. Percentages of lengths of the proestrous stage, estrous stage, and metestrous-diestrous stage to the length of one estrous cycle were calculated for each complete estrous cycle observed for each individual in the 22-day observation. The calculated percentages of lengths of the proestrous stage, estrous stage, and metestrous-diestrous stage to the length of each complete estrous cycle observed in each individual were averaged and are shown in (B), (C), and (D) as one dot. The average of the averaged percentages of length of the proestrous, estrous, and metestrous-diestrous stages to the length of one complete estrous cycle of each WT or *CL* individual is shown in (B), (C), and (D). *CL*, *Clock delta-19* mutants; WT, wild type mice.

isolated, and their body weights were recorded every day at 6 AM. Male mice used in this experiment were removed from the cages 10 days after the appearance of a plug. Recording of body weight and vaginal plugs was continued until Day 27.

The success of copulation was determined by the appearance of a vaginal plug, and the day that a plug was found was defined as the day that copulation had occurred. Pregnancy was monitored by increases in the body weight of female mice. Increases in body weight were calculated by subtracting the body weight on Day 1 of the observation period from the body weight measured on each of the 27 days. Female mice showing a significant increase in body weight compared to the control virgin WT females 17 days after plug formation were defined as pregnant (Fig. 3).

Beginning 17 days after plug formation, a cage was checked three times per day (at 12 AM, 6 AM, and 12 PM) until newborns appeared. At the observation time that the newborns appeared, the number of newborns was determined and recorded as the number of newborns for that female. The day of parturition was defined as the day that newborns appeared. If the delivery was ongoing at the time of the observation, the counting of newborns was delayed until the next observation time. In this study, signs

of cannibalism were not observed in any cage after newborns appeared. One pregnant female in the *CL*♂ × *CL*♀ mating group did not give birth until 24 days after copulation and was euthanized for ethical reasons; this case was counted as delivery failure. In other mating groups, mothers were not harmed or lost by the delivery, and all deliveries were recorded as successful parturitions.

2.4. Perfusion of embryos from oviducts and uteri

Perfusion of embryos was performed according to Hogan et al. [12] with slight modifications. Briefly, 88 hours after fertilization, individual females were sacrificed by cervical dislocation. Each side of the oviduct, right and left, and the uterine horn were collected separately, placed into respective petri dishes, and individually perfused with M2 medium via a syringe [13]. The collected embryos and oocytes were washed twice in a 500-μL drop of fresh M2 medium on a petri dish, and the developmental stage of each was determined via stereomicroscopy. For the sake of convenience, the time of fertilization was defined as midnight (6 PM) of the day before the day that the vaginal plug was found because mice copulate during dark phase of

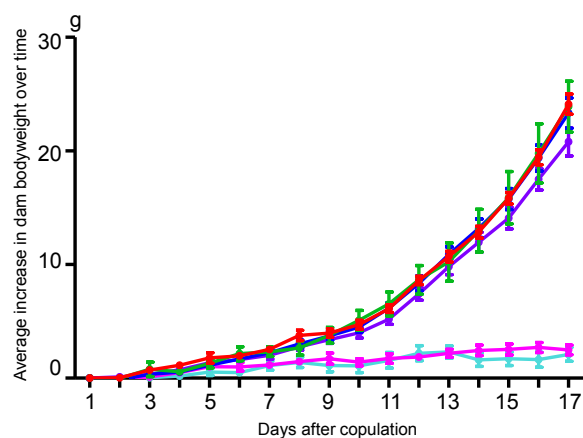


Fig. 3. Change in average body weight increase of dams for each mating group (WT δ × WT ♀ , CL δ × WT ♀ , WT δ × CL ♀ , and CL δ × CL ♀) after copulation. Red line: average change in body weight of pregnant females in the WT δ × WT ♀ group at each observation time, blue line: average change in body weight of pregnant females in the CL δ × WT ♀ group at each observation time, green line: average change in body weight of pregnant females in the WT δ × CL ♀ group at each observation time, violet line: average change in body weight of pregnant females in the CL δ × CL ♀ group at each observation time, pink line: average change in body weight of nonpregnant female *Clock* mutants after copulation at each observation time. Any female mouse that did not show significant increase in body weight compared with the control virgin WT ♀ at 17 days after plug formation was defined as a nonpregnant female. As shown in Table 1, there were three nonpregnant females in the CL δ × CL ♀ group. Light blue line: average change in body weight of virgin female WT ♀ s at each observation time. Analysis of variance followed by Tukey's test was performed to compare the average body weight increases among the mating groups at each observation time. CL, *Clock delta-19* mutants; WT, wild type mice.

a day [12]. The grading of embryos and oocytes was based on Hogan et al. and Cheng et al. [12,14].

2.5. Detection of implantation sites

Detection of implantation sites was performed according to Hogan et al. [12]. Briefly, each pregnant female was anesthetized 160 hours after fertilization via pentobarbital (Somnopenyl, Kyoritsu, Tokyo, Japan). After that, 0.1 mL of a dye solution containing 1% Chicago Sky Blue 6B (C8679; Sigma–Aldrich, St. Louis, MO, USA) dissolved in PBS was injected into the tail vein of a pregnant female mouse; each mouse was then sacrificed exactly 3 minutes after being injected. Immediately after sacrifice, each uterus was collected and extended on filter paper; a picture was taken after the implantation sites had been counted. Digitalization of the distribution of implantation sites in the uterine horns was performed as described by Hama et al. [15] with slight modification. Briefly, a line was drawn from one root of the oviduct to the upper end of the cervix on the picture; this line was divided into two equal parts, an upper part and a lower part (Fig. 4). The number of implantation sites within the upper part of each uterine horn was counted, and the percentage of implantation sites present within the upper uterine horn among all implantation sites was calculated. These percentages were calculated separately for the right and left uterine horns for each female mouse examined. In two female mice in the CL δ × CL ♀ mating

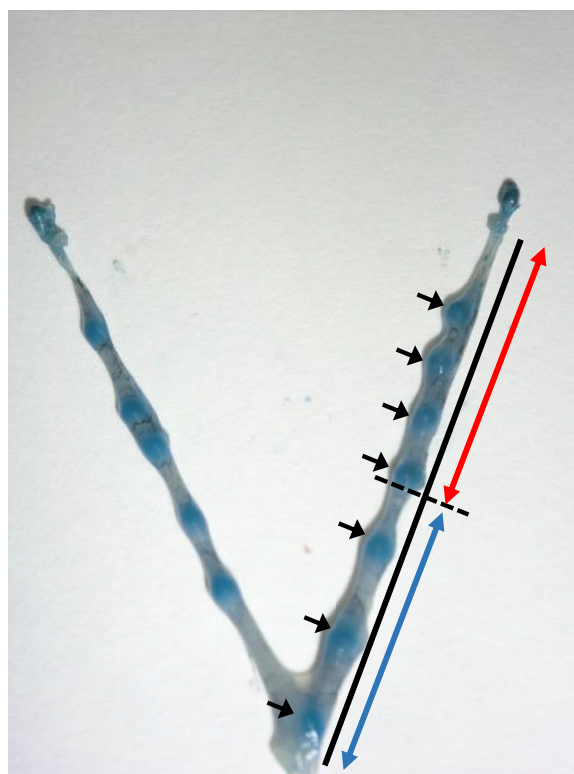


Fig. 4. Representative digitalized image used to determine the distribution of implantation sites in uteri. A line (black line) was drawn from one root of an oviduct to the upper end of the cervix on the picture; this line was divided into two equal parts, an upper part (red arrowhead) and a lower part (blue arrowhead). Each black arrowhead indicates an implantation site. The numbers of the implantation sites were counted separately for the upper and lower parts of each uterine horn, and the percentage of all implantation sites was calculated separately for the upper and the lower uterine horn.

group, one of the uterine horns had implantation sites but the other had no implantation sites. In these two mice, each uterine horn with no implantation sites was excluded from the analysis because we could not determine whether there were no blastocysts at the time of implantation or the blastocysts had difficulty during the implantation process. When an implantation site was at the center of the line that implantation site was counted as being within the uterine part that contained a larger portion of the centrally positioned implantation site.

2.6. Analysis of blastocyst cell number

Each blastocyst comprises an inner cell mass (ICM) cells and trophoblast (TE) cells. To separately count the cell number of ICM cells and TE cells in a blastocyst, we used a previously described double staining technique that employs propidium iodide (PI) and bisbenzimidazole with slight modifications [16]. Briefly, blastocysts were collected from embryos and oocytes that had been perfused from uteri at 88 hours after fertilization [12,14]. Immediately after perfusion, blastocysts were incubated in solution 1 (PBS with 100- μ g/mL PI and 1% Triton X) under a stereomicroscope for 20 to 30 seconds until the color of cells on

the TE side had become red. Next, the blastocysts were incubated in solution 2 (4% paraformaldehyde with 25- μ g/mL bisbenzimidazole [Hoechst 33258]) at 4 °C for 12 hours. The double-stained blastocysts were then mounted onto glass microscope slides with a drop of mounting medium (VECTASHIELD, Vector Laboratories, CA, USA); next, a cover slip was placed on the mounting medium containing the blastocysts. Via this process, the blastocysts were squashed completely onto the glass microscope slide. Only nuclei of TE cells were stained with PI, and nuclei of all cells in the blastocyst were stained with bisbenzimidazole.

The stained blastocysts were observed with an inverted microscope fitted with an ultraviolet lamp and two excitation filters, one for 330 to 385 nm and the other for 520 to 550 nm. The excitation filters for 330 to 385 nm and 520 to 550 nm were used to visualize bisbenzimidazole staining and PI staining, respectively; images of bisbenzimidazole and PI staining were captured and merged. In merged images, the nuclei of TE cells are colored pink because of the double staining with PI and bisbenzimidazole (blue and red, respectively); the nuclei of ICM cells were stained only with bisbenzimidazole and were blue. To count the TE and ICM cells within a blastocyst, the pink-stained nuclei and the blue-stained nuclei were counted separately in the merged photograph. To determine the total cell number of a blastocyst, the TE cell number was added to that of ICM cell number. This figure was rechecked by cross-referencing to the total number of cells in the blastocyst based on counts of blue-stained nuclei in unmerged photographs taken of bisbenzimidazole-stained blastocysts. For this experiment, the numbers of mating pairs prepared for mating groups WT δ \times WT φ , CL δ \times WT φ , WT δ \times CL φ , and CL δ \times CL φ were five, three, five, and three, respectively. From each female mouse used for the analysis, three to five blastocysts were collected. In this case, there was no difference in the developmental rate to the blastocyst stage between these four mating groups, WT δ \times WT φ , CL δ \times WT φ , WT δ \times CL φ , and CL δ \times CL φ .

2.7. Analysis of implanted embryos

Uteri were collected from the females and fixed in Bouin solution at 4 °C. After 12-hour immersion in Bouin solution, each uterus was immersed in 30%, then 80%, and finally 100% ethanol solutions for 1 hour each to dehydrate the tissue. Dehydrated uteri were cleared by immersion in xylene, then xylene/paraffin, and finally paraffin solutions for 1 hour each and were then embedded in paraffin. Each paraffin-embedded uterus was cut into 7-mm sections; these sections were then mounted onto glass slides. To attach sections to the surface of a glass slide, a slide with sectioned tissue was soaked in warm water (42 °C) for 5 seconds. Xylene was used to remove the paraffin from the sections, and each glass slide was briefly immersed in 100%, then 80%, then 30% ethanol solutions, and finally distilled water to rehydrate the tissue. The rehydrated sections were put into hematoxylin solution and then eosin solution for 20 seconds each. After washing with distilled water, the slides were immersed in 30%, then 80%, and finally 100% ethanol solutions to dehydrate the tissue again; sections

were then washed with xylene. The stained sections were mounted using mounting solution (1079610100; Entellan new, Merck, NJ, USA) and observed via a stereomicroscopy. One female from the WT δ \times WT φ mating group and two females from the CL δ \times CL φ mating group were used in this experiment. From each female mouse, one of the uterine horns, which generally included 4 to 5 implantation sites, was collected. All the implantation sites included in the specimen were sectioned and analyzed, and representative pictures are shown in this article.

2.8. Statistical analysis

Data from the experiments were analyzed by Student *t* test, the X^2 test, or analysis of variance (ANOVA) followed by Tukey's test. Before Student *t* test, the *f* test was conducted to check the homogeneity of the variance across the data from each experiment. Before ANOVA and Tukey's test, Bartlett's test was conducted to check the homogeneity of the variance across the data from each experimental group. If the homogeneity of the variance was rejected, the Steel-Dwass test was performed. Detailed explanations of statistical analysis are provided in the respective figure legends or the notes for the respective table.

3. Results

3.1. Effect of CL on estrous cycle progression

The average numbers of estrous cycles in WT and female CL mice during the observation period were 3.0 ± 0.2 and 2.7 ± 0.2 , respectively; this difference was not statistically significant. Similarly, average total length of the estrous cycle did not differ significantly between WT mice and CL mice (5.4 ± 0.3 vs. 5.2 ± 0.2 days, respectively). The average lengths of the proestrous stage, estrous stage, and metestrous-diestrous stage in CL mice were 1.1 ± 0.1 days, 1.8 ± 0.2 days, and 2.5 ± 0.2 days, respectively, and those of WT were 1.1 ± 0.1 days, 2.0 ± 0.1 days, and 2.3 ± 0.2 days, respectively. For each stage of the estrous cycle, the WT mice and CL mice did not differ significantly (Table 1 and Fig. 1). For reducing the possibility that the difference in the number of complete estrous cycles between the animals affects the results, the length of one complete estrous cycle and the percentages of the lengths of the proestrous stage, estrous stage, and metestrous-diestrous stage to the length of one complete estrous stage were averaged for each individual and compared between WT and CL mice. However, no differences were observed in the length of the estrous cycle and the percentages of the lengths of the proestrous stage, estrous stage, and metestrous-diestrous stage between WT and CL mice (Fig. 2).

3.2. Effect of CL on reproductive performance

Copulation was observed in each mating group (WT δ \times WT φ , CL δ \times WT φ , WT δ \times CL φ , and CL δ \times CL φ), and the period from the start of cohabitation to copulation did not differ significantly among the mating groups. The proportions of pregnant females and of pregnant

Table 2

Comparison of reproduction profiles among the four mating groups: WT♂ × WT♀, CL♂ × WT♀, WT♂ × CL♀, and CL♂ × CL♀.

Reproductive profile components	WT♂ × WT♀	CL♂ × WT♀	WT♂ × CL♀	CL♂ × CL♀
Number of examined mating pairs	14	10	14	15
Number of mating pairs exhibiting successful copulation (%)	14 (100)	10 (100)	14 (100)	15 (100)
Average period from the start of mating to the day of copulation (days ± SEM)	2.4 ± 0.3	3.0 ± 0.6	2.8 ± 0.4	3.1 ± 0.5
Number of mating pairs with a pregnant female (number of mating pairs with a pregnant female/number of examined mating pairs, %) ^a	14 (100)	10 (100)	14 (100)	12 (80.0)
Number of pregnant females exhibiting successful delivery (number of the pregnant females with successful delivery/number of mating pairs with a pregnant female, %)	14 (100)	10 (100)	14 (100)	11 (91.7)
Average number of days from copulation to parturition ± SEM ^b	19.3 ± 0.2 ^A	19.1 ± 0.2 ^A	19.8 ± 0.2 ^{AB}	20.5 ± 0.5 ^B
Average number of newborns immediately after birth ± SEM ^c	13.4 ± 0.8 ^A	12.6 ± 0.4 ^A	12.3 ± 0.7 ^A	8.6 ± 1.5 ^B

Values with different superscript uppercase letters and in the same row differ significantly from each other.

Abbreviations: CL, *Clock delta-19* mutants; SEM, standard error of the mean; WT, wild type mice.

^a Each female mouse that showed a significant increase in body weight compared to the control virgin WT♀ at 17 days after plug formation was defined as pregnant.

^b The average period from copulation to parturition and average number of newborns were calculated using only data obtained from mating pairs involving pregnant females that delivered successfully.

^c Comparisons among data obtained from the four mating groups (WT♂ × WT♀, CL♂ × WT♀, WT♂ × CL♀ and CL♂ × CL♀) were performed via analysis of variance followed by Tukey's test. The X² test was performed for comparison among mating groups with regard to the numbers of the mating pairs with a pregnant female and the number of pregnant females that successfully delivered.

females who delivered successfully did not differ significantly among the mating groups (Table 2). However, the average period from copulation to parturition was longer when the female parent or both parents were homozygous for CL. The average copulation-to-parturition period was significantly longer for the CL♂ × CL♀ group than that for each other mating group except WT♂ × CL♀ (19.3 ± 0.2 days, 19.1 ± 0.2 days, 19.8 ± 0.2 days, and 20.5 ± 0.5 days, $P < 0.05$, Table 2). The number of newborns for the CL♂ × CL♀ group was the lowest of all groups and significantly different from the numbers in the other groups (13.4 ± 0.8, 12.6 ± 0.4, 12.3 ± 0.7, and 8.6 ± 1.5, $P < 0.05$, Table 2).

3.3. Effect of CL on body weight increase during pregnancy

To assess potential fetal loss or spontaneous abortion during mid gestation, profiles of increases in body weight of female mice after copulation were examined. Increases in individual body weights of pregnant females did not differ significantly among the mating groups. In addition, the profile of increases in body weight of nonpregnant females in the CL♂ × CL♀ group was the same as that for virgin control WT females (Fig. 3). Taken together, the data suggested that pregnant ICR CL mice did not lose their fetuses during mid gestation. Although increases in body weight only indirectly reflect the state of pregnancy, our findings differed from previously published findings [10]. Therefore, we next focused on the effects of CL on early embryonic development.

3.4. Effect of CL on the development of early embryos

The average number of embryos collected from each mating group (WT♂ × WT♀, CL♂ × WT♀, WT♂ × CL♀, and CL♂ × CL♀) did not differ significantly among the groups (Table 3). We assessed six early developmental stages—oocyte (1-cell), 2-cell, 4-cell, 8-cell, 16-cell to morula, and

blastocyst—to determine proportions of individuals at each stage among all individuals (Fig. 5). The proportion of embryos at the 16-cell to morula stage was higher among embryos bearing one or two CL alleles than among homozygous WT embryos, and there was a significant difference between the WT♂ × WT♀ and CL♂ × CL♀ groups with regard to the proportion of embryos that reached the 16-cell to morula stage (Fig. 5, $P < 0.05$). However, proportions of embryos that reached each other stage (except for the 16-cell to morula stage) did not differ significantly among the mating groups. In this experiment, we could not distinguish the fertilized oocytes that remained uncleaved from the unfertilized oocytes. For this reason, the zygotes or oocytes that had not undergone cleavage were classified as “unfertilized oocytes or 1-cell zygotes” in this study.

3.5. Effect of CL on implantation

The average number of implantation sites per mating was significantly lower for the CL♂ × CL♀ group than that for any other group ($P < 0.05$, Table 4). Notably, a significantly larger proportion of implantation sites was located in the lower part of the uterine horn for the CL♂ × WT♀ or WT♂ × CL♀ group than that in the WT♂ × WT♀ group ($P < 0.05$, Figs. 6 and 7). This abnormal positioning of implantation sites in the uterus was more severe for the WT♂ × CL♀ group than for the CL♂ × WT♀ group, and this abnormal positioning was most severe in the CL♂ × CL♀ group (Figs. 6 and 7). However, the data from the CL♂ × CL♀ group were excluded from the statistical analysis because the total number of implantation sites in CL♂ × CL♀ mating group was significantly smaller than the numbers in other mating groups and because this small sample size caused greater variation in the CL♂ × CL♀ data compared to data from the other mating groups. Consequently, the CL♂ × CL♀ data were not suitable for a statistical comparison with data from other mating groups ($P < 0.05$, Table 4).

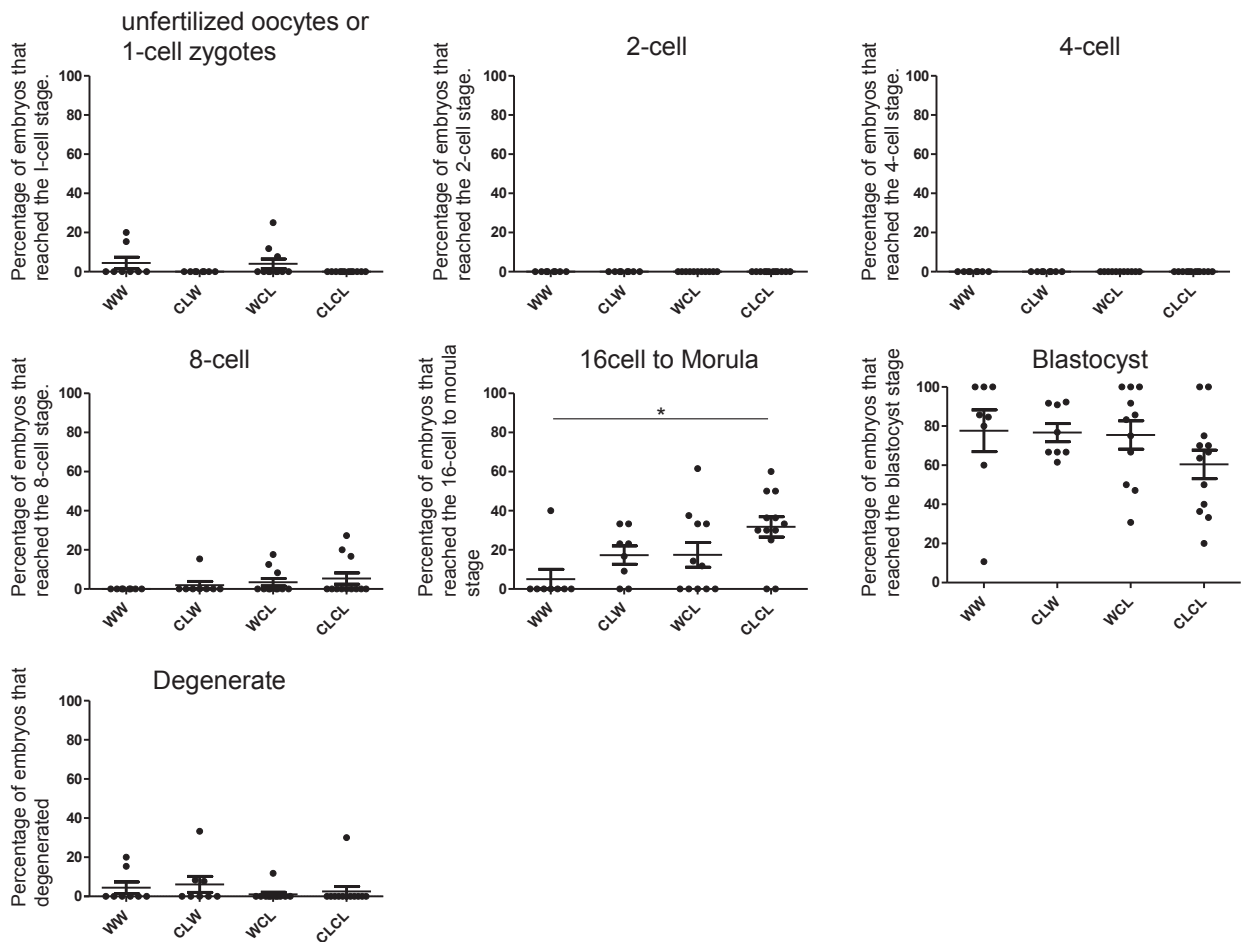


Fig. 5. Developmental stages of embryos collected from the four mating groups ($WT\delta \times WT\varnothing$, $CL\delta \times WT\varnothing$, $WT\delta \times CL\varnothing$, and $CL\delta \times CL\varnothing$) 88 hours after fertilization. WW, CLW, WCL, and CLCL indicate the mating groups $WT\delta \times WT\varnothing$, $CL\delta \times WT\varnothing$, $WT\delta \times CL\varnothing$, and $CL\delta \times CL\varnothing$, respectively. The developmental stages that were scored in this experiment were unfertilized oocytes or 1-cell zygotes, 2-cell, 4-cell, 8-cell, morula, and blastocyst. Degenerate indicates the rates of the embryos with abnormal morphology in each mating group [12,14]. Each dot in each graph represents data from a single dam. The middle bars shown in each column represent the averaged developmental rates in each mating group. Each error bar represents an SEM. Analysis of variance followed by Tukey's test was done to compare the average developmental rates between the mating groups. Asterisk shows the statistically significant difference between each group.

3.6. Comparison between WT blastocysts and homozygous CL blastocysts with regard to total blastocyst cell number and to the ratio of ICM cells to all cells in a blastocyst

Based on published data, each embryo with a blastocoel 88 hours after fertilization was classified as a blastocyst-stage embryo for our study [12,14]. However, CL could potentially affect blastocyst quality, total cell number within the blastocysts, ratio of ICM cells to all cells within blastocysts, or some combination thereof regardless of the presence of a blastocoel. To investigate these possibilities, blastocysts resulting from $WT\delta \times WT\varnothing$, $CL\delta \times WT\varnothing$, $WT\delta \times CL\varnothing$, or $CL\delta \times CL\varnothing$ pairings were collected 88 hours after fertilization, and double staining with bisbenzimidazole and PI was used to compare the groups with regard to total blastocyst cell number and ratio of ICM cell number to total cell number (Fig. 8). The mean total cell number and mean ratio of ICM-to-total cell number for blastocysts from the $WT\delta \times WT\varnothing$, $CL\delta \times WT\varnothing$, or $WT\delta \times CL\varnothing$ groups did

not differ statistically, but each was significantly larger than those of blastocysts from the $CL\delta \times CL\varnothing$ group ($P < 0.05$, Table 5).

3.7. Comparison between WT embryos and homozygous CL embryos with regard to morphology of implantation sites

Around the time of implantation, blastocysts are positioned at implantation sites and are adjusted such that the trophoblast apposes the uterine epithelium [17]. Because the mechanisms driving these movements are regulated by embryonic and uterine factors, uterine and/or embryonic CL mutation could potentially cause morphologic abnormality or the loss of embryos at the implantation site [17–19]. To investigate this possibility, the $WT\delta \times WT\varnothing$ and $CL\delta \times CL\varnothing$ groups were compared with regard to the morphology of implantation sites in cross-sections of uterine tissue collected 160 hours after copulation. Differences in the morphology of implantation sites were

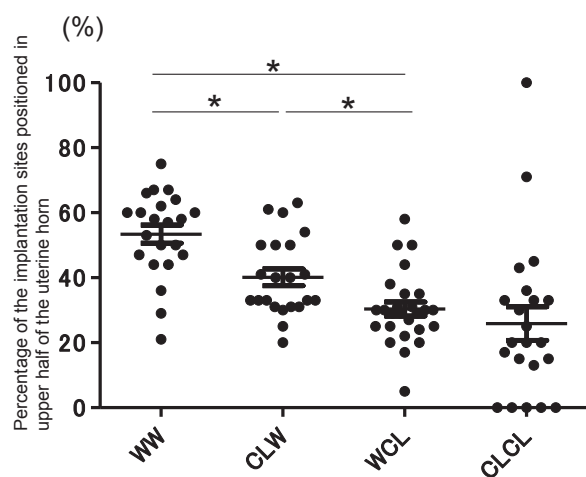


Fig. 6. Proportion of implantation sites observed in the upper part of the uterine horns at 160 hours after copulation. WW, CLW, WCL, and CLCL indicate the mating groups WT δ × WT φ , CL δ × WT φ , WT δ × CL φ , and CL δ × CL φ , respectively. Analysis of variance followed by Tukey's test was done to detect statistical differences between mating groups with regard to average proportion of all implantation sites located in the upper part of the respective uterine horn. The data from the CL δ × CL φ group were excluded from statistical analysis because the total number of implantation sites in the CL δ × CL φ mating group was significantly lower than that for the other mating groups; therefore, comparisons involving the CL δ × CL φ data would not have been statistically valid ($P < 0.05$, Table 4). Each middle bar shown in each data column represents the average percentage of all embryos in the respective horn present in the upper side of the respective horn. Each error bar represents an SEM. Asterisk shows the statistically significant difference between each group. CL, *Clock delta-19* mutants; WT, wild type mice.

not evident between the WT δ × WT φ and CL δ × CL φ groups (Fig. 9).

4. Discussion

In this study, we showed that among all events that occur from fertilization to parturition, CL primarily affects the success of implantation. Furthermore, we obtained results suggesting that embryonic CL, like maternal CL, affects the implantation process.

CL female mice had normal estrous cycles and the same opportunity to deliver pups as did WT females (Table 1 and Figs. 1 and 2); therefore, we compared the reproductive profiles of four mating groups—WT δ × WT φ , CL δ × WT φ , WT δ × CL φ , and CL δ × CL φ —in this study. In our study, CL greatly affected the number of newborns (Table 2), and this effect was thought to be due to fetal loss very early in gestation (0–5 days after fertilization); this finding differed from a previous finding (Fig. 3) [10]. Moreover, CL did not affect embryonic development to the blastocyst stage; however, if either of or both parents were homozygous for CL, the position of implantation sites was abnormally lowered in the uterus, and the number of implantation sites was smaller (Tables 3 and 4, Figs. 5–7). Together, these findings suggested that CL affected implantation. On the other hand, the capacity for copulation of either CL δ or CL φ was assumed to be normal because the period from the start of cohabitation to the day of copulation did not differ significantly among the mating groups (Table 2). Moreover,

the ejaculation capacity of CL δ , fertilization capacity of CL δ spermatozoa and of CL φ oocytes, and the number of ovulated CL φ oocytes apparently did not differ from those of WT δ or WT φ because the total number of obtained oocytes and embryos and the percentage of embryos among all obtained oocytes and embryos at 88 hours after copulation did not differ significantly among the mating groups (Table 3).

The distribution of implantation sites observed in the CL δ × WT φ mating group was significantly lower in the uterus than that in the WT δ × WT φ mating group (Fig. 6, $P < 0.05$), and this difference was thought to depend on the difference in embryonic genotype, specifically between homozygous WT and heterozygous embryos. However, the distribution of implantation sites observed in the WT δ × CL φ mating group was significantly lower than that in the CL δ × WT φ group (Fig. 6, $P < 0.05$); this difference was thought to depend on the difference in maternal genotype, specifically between homozygous WT and homozygous mutant dams. Consequently, we concluded that the abnormal positioning of the implantation sites could be caused by either maternal or embryonic CL.

In our study, statistically significant reductions in the numbers of newborns and implantation sites were only observed for the CL δ × CL φ group (Tables 2 and 4, $P < 0.05$). For the CL δ × WT φ and WT δ × CL φ groups, it can be speculated that the perturbation of distribution of the implantation sites was comparatively moderate and resulted in a normal number of implantation sites that was similar to the number for the WT δ × WT φ group. However, for the CL δ × CL φ group, it is speculated that the additive effects of CL in both mothers and embryos severely perturbed the distribution of implantation sites and therefore reduced the numbers of implantation sites and newborns.

From 96 to 108 hours after fertilization, the mouse uterus is primed for implantation via progesterone secreted from the corpus luteum [20]. Several studies have indicated that mice bearing this specific CL mutation (*Clock delta-19*) or an *Arntl* deficiency have reduced or mistimed secretion of progesterone from the corpus luteum during the implantation window, and it may be that perturbation of progesterone secretion in homozygous CL mothers caused the reduction in implantation sites in the uteri (Table 2 and Figs. 6 and 7) [10,21]. On the other hand, female mice bearing a deficiency of lysophosphatidic acid 3 (*LPA3*) or cytosolic phospholipase A2 α (*cPLA2 α*) show phenotypes resembling those observed in any mating group involving CL mice in our study; specifically, crowding of implantation sites in the lower part of the uterus and reduction in the number of implantation sites were observed when WT blastocysts were implanted [18,19]. Because both *LPA3* and *cPLA2 α* are necessary for the synthesis of prostaglandins required for implantation, *Clock* might promote implantation by being involved in the mechanisms for synthesis of prostaglandins regardless of whether or not *Clock* is involved in the synthesis and/or secretion of *LPA3* and *cPLA2 α* . On the other hand, in those studies, supplementation of prostaglandins to the pregnant female mice bearing deficiency of *LPA3* or *cPLA2 α* around the preimplantation stage did not improve the crowding of implantation sites; these findings suggest that *LPA3* and *cPLA2 α*



Fig. 7. Representative images of uteri collected from the indicated mating groups ($WT\delta \times WT\eta$, $CL\delta \times WT\eta$, $WT\delta \times CL\eta$, or $CL\delta \times CL\eta$) 160 hours after fertilization. Each arrowhead indicates a stained implantation site. *CL*, *Clock delta-19* mutants; *WT*, wild type mice.

regulate spacing of the implantation sites via mechanisms other than secretion of prostaglandins and that *Clock* is involved in the functions of a gene group that include *LPA3* and *cPLA2 α* , which regulate the spacing of the embryos in the uterus via mechanisms other than producing prostaglandins. Moreover, in those studies, supplementation of prostaglandins increased the number of implantation sites in females bearing a deficiency of *LPA3* or *cPLA2 α* , but the number of implantation sites was not fully recovered to the level observed in *WT* females; these findings suggest that crowding of the implantation sites increases implantation failure.

Based on published findings, each embryo with a blastocoel at 88 hours after fertilization was classified as a blastocyst-stage embryo in our study [12,14]. In our study, the percentage of embryos that developed to the blastocyst stage among all embryos did not differ significantly among the mating groups; therefore, *CL* in blastocysts was assumed to potentially affect implantation via a mechanism other than those mechanisms that affect embryonic cell proliferation or differentiation. However, embryonic *CL* could have potentially affected blastocyst quality, ratio of ICM number to total cell number in a blastocyst, implantation capacity, or some combination thereof. To gain more insights into the role of embryonic *CL* in implantation, we analyzed total cell number and percentage of ICM cells among all cells within blastocysts

derived for each mating group, $WT\delta \times WT\eta$, $CL\delta \times WT\eta$, $WT\delta \times CL\eta$, or $CL\delta \times CL\eta$. Because the quality of the blastocysts derived from $WT\delta \times WT\eta$, $CL\delta \times WT\eta$, or $WT\delta \times CL\eta$ pairs did not differ significantly, the observed difference between $WT\delta \times WT\eta$ and $CL\delta \times WT\eta$ pairs with regard to the positioning of implantation sites was thought to be due to the effect of *CL* in blastocysts, but *CL* in blastocysts was assumed to potentially affect the implantation via a mechanism other than embryonic cell proliferation or differentiation. As far as we know, no published reports have shown that blastocyst factors can cause the phenotype observed in the $CL\delta \times WT\eta$ mating group, specifically crowding of implantation sites in the lower part of the uterus. However, implantation involves cross talk between the uterus and blastocysts; therefore, blastocyst *Clock* might modulate uterine factors such as *LPA3* and *cPLA2 α* , which are known to promote normal spacing and implantation, by affecting secretion from blastocysts of some substances that affect uterine physiology. Our data showed that quality of the blastocyst and the ratio of ICM cell number to total cell number in a blastocyst derived from $CL\delta \times CL\eta$ mating pairs were lower than those derived from the other mating groups (Table 5). Although this result might be due to the fluctuation of copulation and/or the fertilization time in the mating group of $CL\delta \times CL\eta$, it was also possible that embryonic *CL* was involved in the proliferation and/or the differentiation of embryonic cells.

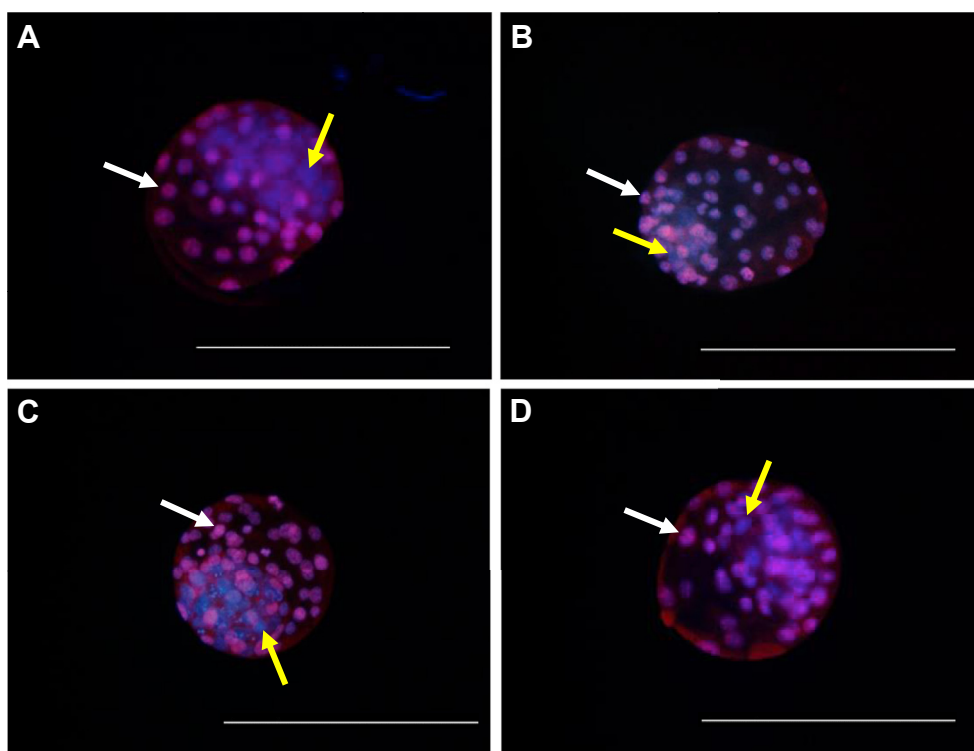


Fig. 8. Panels (A), (B), (C), and (D) are the images of typical blastocysts derived from the $WT\delta \times WT\delta$, $CL\delta \times WT\delta$, $WT\delta \times CL\delta$, and $CL\delta \times CL\delta$ groups, respectively. The intense pink-colored spots represent TE cell nuclei that were stained with both PI and bisbenzamide (white arrowhead). The blue spots (yellow arrowhead) represent nuclei of ICM cells. Scale bar = 200 μm . CL, *Clock delta-19* mutants; ICM, inner cell mass; PI, propidium iodide; TE, trophoblast; WT, wild type mice.

However, the blastocyst quality was the same in $WT\delta \times WT\delta$ mating pairs, which produced WT blastocysts, and in $CL\delta \times WT\delta$ and $WT\delta \times CL\delta$ pairs, which produced heterozygous CL blastocysts; these findings suggested that the effect of embryonic CL on cell proliferation and/or differentiation in embryos might be small (Table 5).

The data obtained in our study showed that CL in the mother was not the only factor causing a defect in implantation and the results suggested that embryonic CL also affected implantation ability (Tables 2–5, Figs. 5–7). However, the impact of embryonic CL on implantation still needs to be carefully examined by further studies including an implantation test of WT/CL embryos on cultured WT/CL endometrium cells and/or a comparison of the ratios of the number of heterozygous CL offspring and CL offspring between mating of male CL and heterozygous female CL and mating of heterozygous male CL and female CL.

Around the time of implantation, blastocysts are positioned at implantation sites, and embryonic position is adjusted such that the trophoblast apposes the uterine epithelium [17]. Because the mechanisms driving these movements are regulated by embryonic and uterine factors, uterine and/or embryonic CL could potentially cause morphologic abnormalities at implantation sites [17–19]. However, based on our analysis of implantation sites 160 hours after fertilization, there were no morphological differences between the $WT\delta \times WT\delta$ and $CL\delta \times CL\delta$ mating groups that indicated embryonic loss or displaced implantation (Fig. 9).

The gestation period was significantly longer when both parents were homozygous for CL (Table 2, $P < 0.05$), although a slight elongation was also observed when only the mother was homozygous for CL; these findings indicated that both maternal CL alleles and embryonic CL alleles affected the gestation period. Parturition is a typical circadian phenomenon that tends to occur at a particular time during the day, and although there was a possibility that the decreased number of fetuses affected the length of the gestation period in CL mice, perturbation of the mother's circadian clock by CL might have affected the daily activation of some parturition-inducing factors (e.g., oxytocin secretion) that appear only in the few days near the end of the gestation period (around Day 19), and such perturbations may have caused the elongation of the gestation period [21–23]. On the other hand, in sheep, when the hypothalamus-pituitary-adrenal axis of a fetus has matured, cortisol is secreted from the fetal adrenal gland and triggers many events necessary for parturition, including decreased secretion of progesterone from the placenta [20,24]. It is likely that the maternal CL alleles delayed the development of the hypothalamus-pituitary-adrenal axis of fetal mice and/or that the CL alleles in the fetal mice affected the function of the fetal hypothalamic-pituitary-adrenal axis [17,20,24,25].

Miller et al. [10] reported a severe reduction in production of newborns in the C57/BL6 inbred strain bearing this CL (*Clock delta-19*). They found that female mice bearing CL exhibit an abnormally elongated estrous

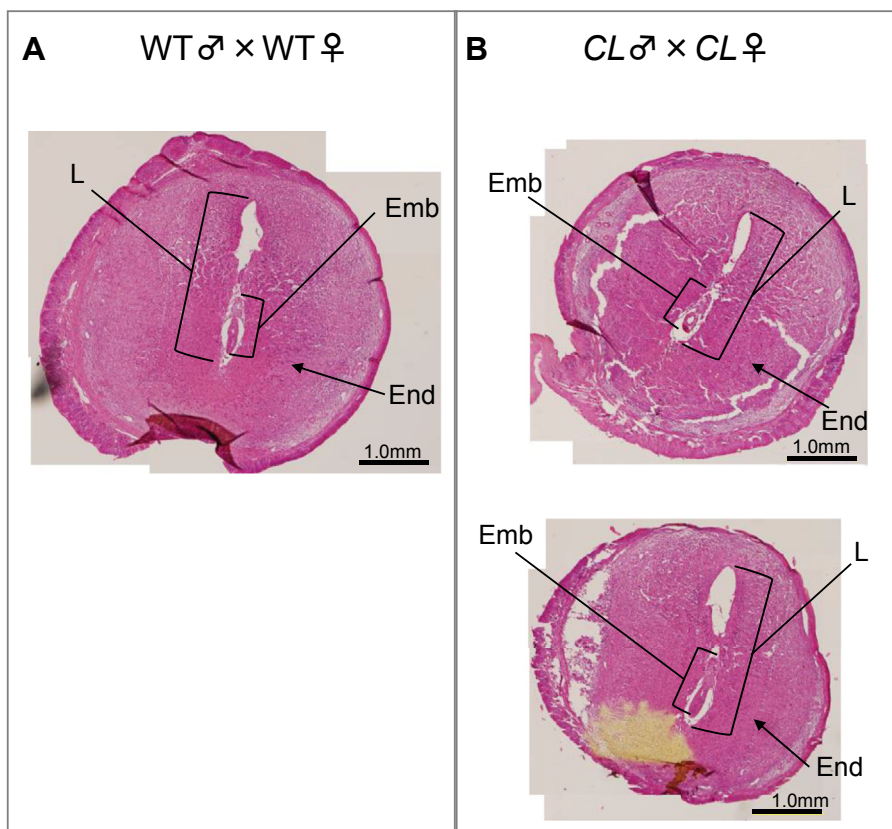


Fig. 9. Sections of implantation sites from females in the WT♂ × WT♀ and CL♂ × CL♀ groups; uteri were collected 160 hours after fertilization. (A) Typical morphology of an implantation site derived from the WT♂ × WT♀ group. (B) Typical morphologies of implantation sites derived from the CL♂ × CL♀ group. Two pictures were taken to represent the CL♂ × CL♀ group; these pictures were from different dams. The sections were stained with hematoxylin and eosin. Notably, the morphologies of the implantation sites did not differ between these two mating groups, WT♂ × WT♀ and CL♂ × CL♀, and embryonic loss or displaced implantation was not observed in the implantation sites in the CL♂ × CL♀ mating group. CL, *Clock delta-19* mutants; Emb, embryo; End, endometrium; L, lumen; WT, wild type mice.

stage and become pregnant, but these pregnancies result in very few live newborns because fetuses are reabsorbed during the mid-gestational stage (11–14 days after copulation). However, we did not observe an elongated estrous stage or any sign of fetal loss around mid-gestation or at

Table 3
Comparison of the number of embryos collected 88 hours after fertilization among the four mating groups: WT♂ × WT♀, CL♂ × WT♀, WT♂ × CL♀, and CL♂ × CL♀.

Mating groups	Number of examined mating pairs	Number of mating pairs with no embryos	Average number ± SEM of embryos/mating pair
WT♂ × WT♀	8	0	11.4 ± 1.5
CL♂ × WT♀	8	0	12.0 ± 0.5
WT♂ × CL♀	11	0	10.6 ± 1.0
CL♂ × CL♀	11	0	10.7 ± 0.8

The time of copulation was set to 0:00 of the day that a plug was observed. A vaginal plug was observed in each female mouse of an examined mating. Statistical comparison among the mating groups—WT♂ × WT♀, CL♂ × WT♀, WT♂ × CL♀, and CL♂ × CL♀— was performed via analysis of variance followed by Tukey's test.

Abbreviations: CL, *Clock delta-19* mutants; SEM, standard error of the mean; WT, wild type mice.

Table 4
Comparison of the number of implantation sites in uteri that were collected 160 hours after fertilization among the four mating groups: WT♂ × WT♀, CL♂ × WT♀, WT♂ × CL♀, and CL♂ × CL♀.

Mating groups	Number of examined mating pairs	Number of mating pairs with no evidence of an implantation site (%)	Average number ± SEM of implantation sites/mating pair
WT♂ × WT♀	12	1 (8.3)	13.0 ± 1.5 ^A
CL♂ × WT♀	11	0 (0.0)	13.1 ± 1.2 ^A
WT♂ × CL♀	13	0 (0.0)	11.7 ± 0.8 ^A
CL♂ × CL♀	13	1 (7.1)	7.0 ± 1.3 ^B

The time of copulation was set to 0:00 of the day that a plug was observed. A vaginal plug was observed in each female mouse of an examined mating pair.

Statistical comparisons among the mating groups—WT♂ × WT♀, CL♂ × WT♀, WT♂ × CL♀, and CL♂ × CL♀— were performed via analysis of variance followed by Tukey's test.

Values with different superscript uppercase letters and in the same column differ significantly from each other. For calculation of average number ± SEM of implantation sites/mating pair, the pairs with no evidence of an implantation site were omitted.

Abbreviations: CL, *Clock delta-19* mutants; SEM, standard error of the mean; WT, wild type mice.

Table 5

Comparisons of total cell numbers and percentage of ICM cell numbers/total cell numbers of blastocysts collected 88 hours after fertilization among the four mating groups: WT♂ × WT♀, CL♂ × WT♀, WT♂ × CL♀, and CL♂ × CL♀.

Mating groups	Number of examined mating pairs ^a	Number of examined blastocysts	Median of total cell number ^b	25% percentile of total cell number ^b	75% percentile of total cell number ^b	ICM cell number/total cell number (%) ^c
WT♂ × WT♀	5	22	60	50.8	65.3	28.4 ± 2.5 ^A
CL♂ × WT♀	3	13	50	39.0	61.5	19.6 ± 3.2 ^A
WT♂ × CL♀	5	23	46	37.5	62.5	22.1 ± 1.9 ^A
CL♂ × CL♀	3	10	56	49.5	59.0	13.8 ± 2.9 ^B

Values with different superscript uppercase letters and in the same row differ significantly from each other.

Abbreviations: CL, *Clock delta-19* mutants; ICM, inner cell mass; WT, wild type mice.

^a Three to five blastocysts were analyzed for each mating.

^b Total cell number data are expressed as medians and 25 to 75 percentiles; statistical analysis was performed with the Steel-Dwass test.

^c Statistical comparison of the data for ICM cell number/total cell number (%) was performed via analysis of variance followed by Tukey's test.

full-term in homozygous *CL* dams (Table 1 and Figs. 1–3). These differences between our ICR *CL* mice and the C57/BL6 *CL* homozygote mutants were thought to be due to differences in genetic backgrounds of the two strains. Under the condition of constant darkness, the daily rhythm in locomotor activity in *CL* mice with the ICR background continues for 2 months; however, the cycle length is elongated. In contrast, *CL* mice with the BALB/cj and C57/BL/6J background become arrhythmic within just 5 to 15 twenty-four-hour cycles. These findings suggest that *CL* has a milder effect on ICR mice than on C57/BL6 mice [8,26]. Moreover, our data resembled previous data showing that female ICR mice bearing *CL* produce fewer newborns than do wild-type dams; however, the reduction in the number of newborns (35.8%) was larger in our study than that in the previous study, in which there was a reduction of 10% (Table 2) [6].

Although the number of newborns was significantly smaller for the CL♂ × CL♀ group than that for the other mating groups, the average body weight of pregnant females did not differ significantly among the groups (Table 2 and Fig. 3). This observation might be explained by a well-known phenomenon in mice; specifically, the body sizes of individual fetuses and the amount of amniotic fluid decrease as the total number of fetuses/uterus increases [27,28].

In this study, we used the ICR strain of mice because it has higher genetic variation than do individual inbred strains, and it can serve as a better model for humans and domestic animal populations. We used eight to 15 ICR mice for each treatment group in each experiment, and this number of mice was sufficient to detect statistically significant effects of *CL* on traits such as (1) the period from copulation to parturition, (2) the distribution of implantation sites, and (3) the number of implantation sites and number of newborns. That this small sample size could give rise to statistically significant results indicated that that differences among phenotypes observed in our study can appear in groups of humans or domestic animals with similar frequencies. Thus, our data suggest the importance of the circadian clock for reproductive health in humans and productivity of domestic animals and fowls.

In summary, we demonstrated that not only maternal *CL* but also factors other than maternal *CL* such as embryonic *CL* are involved in reproductive performance of mice because of the effects on implantation.

Acknowledgments

This work was supported by a grant from the Kanzawa Medical Research Foundation, a Grant-in-Aid for Young Scientists (23780280), and a Grant-in-Aid for Scientific Research (26450383) from the Japanese Ministry of Education, Culture, Sports, and Technology. The funding sources had no involvement in study design, data collection, data analysis, data interpretation, or writing of the article.

Competing interests

The authors declare no conflict of interest associated with this article.

References

- [1] Albrecht U. Invited review: regulation of mammalian circadian clock genes. *J Appl Physiol* 2002;92:1348–55.
- [2] King DP, Takahashi JS. Molecular genetics of circadian rhythms in mammals. *Annu Rev Neurosci* 2000;23:713–42.
- [3] Reppert SM, Weaver DR. Coordination of circadian timing in mammals. *Nature* 2002;418:935–41.
- [4] Ko CH, Takahashi JS. Molecular components of the mammalian circadian clock. *Hum Mol Genet* 2006;15:R271–7.
- [5] Harmer SL, Panda S, Kay SA. Molecular bases of circadian rhythms. *Annu Rev Cell Dev Biol* 2001;17:215–53.
- [6] Hoshino K, Wakatsuki Y, Iigo M, Shibata S. Circadian Clock mutation in dams disrupts nursing behavior and growth of pups. *Endocrinology* 2006;147:1916–23.
- [7] Ochi M, Sono S, Sei H, Oishi K, Kobayashi H, Morita Y, et al. Sex difference in circadian period of body temperature in Clock mutant mice with Jcl/ICR background. *Neurosci Lett* 2003;347:163–6.
- [8] Oishi K, Miyazaki K, Ishida N. Functional CLOCK is not involved in the entrainment of peripheral clocks to the restricted feeding: entrainable expression of mPer2 and BMAL1 mRNAs in the heart of Clock mutant mice on Jcl: ICR background. *Biochem Biophys Res Commun* 2002;298:198–202.
- [9] Sei H, Oishi K, Morita Y, Ishida N. Mouse model for morningness/eveningness. *Neuroreport* 2001;12:1461–4.
- [10] Miller BH, Olson SL, Turek FW, Levine JE, Horton TH, Takahashi JS. Circadian clock mutation disrupts estrous cyclicity and maintenance of pregnancy. *Curr Biol* 2004;14:1367–73.
- [11] Dolatshad H, Campbell E, O'hara L, Maywood E, Hastings M, Johnson M. Developmental and reproductive performance in circadian mutant mice. *Hum Reprod* 2006;21:68–79.
- [12] Hogan B, Costantini F, Lacy E. *Manipulating the mouse embryo: a laboratory manual*. Cold Spring Harbor, NY: Cold spring harbor laboratory; 1986.
- [13] Quinn P, Barros C, Whittingham D. Preservation of hamster oocytes to assay the fertilizing capacity of human spermatozoa. *J Reprod Fertil* 1982;66:161–8.
- [14] Cheng T, Huang C, Huang L, Chen C, Lee M, Liu J. Evaluation of mouse blastocyst implantation rate by morphology grading. *Chin J Physiol* 2004;47:43.

- [15] Hama K, Aoki J, Inoue A, Endo T, Amano T, Motoki R, et al. Embryo spacing and implantation timing are differentially regulated by LPA3-mediated lysophosphatidic acid signaling in mice. *Biol Reprod* 2007;77:954–9.
- [16] Thouas G, Korfiatis N, French A, Jones G, Trounson A. Simplified technique for differential staining of inner cell mass and trophoctoderm cells of mouse and bovine blastocysts. *Reprod Biomed Online* 2001;3:25–9.
- [17] Chen Q, Zhang Y, Elad D, Jaffa AJ, Cao Y, Ye X, et al. Navigating the site for embryo implantation: biomechanical and molecular regulation of intrauterine embryo distribution. *Mol Aspects Med* 2013;34:1024–42.
- [18] Ye X, Hama K, Contos JJ, Anliker B, Inoue A, Skinner MK, et al. LPA3-mediated lysophosphatidic acid signalling in embryo implantation and spacing. *Nature* 2005;435:104–8.
- [19] Song H, Lim H, Paria B, Matsumoto H, Swift L, Morrow J, et al. Cytosolic phospholipase A2alpha is crucial [correction of A2alpha deficiency is crucial] for 'on-time' embryo implantation that directs subsequent development. *Development* 2002;129:2879–89.
- [20] Sudhansu D, Hyunjung L. *Physiology of Reproduction* 3rd edition. Cambridge, MA: Academic Press; 2006.
- [21] Ratajczak CK, Boehle KL, Muglia LJ. Impaired steroidogenesis and implantation failure in *Bmal1*^{-/-} mice. *Endocrinology* 2009;150:1879–85.
- [22] Bossmar T, Åkerlund M, Fantoni G, Szamatowicz J, Melin P, Maggi M. Receptors for and myometrial responses to oxytocin and vasopressin in preterm and term human pregnancy: effects of the oxytocin antagonist atosiban. *Am J Obstet Gynecol* 1994; 171:1634–42.
- [23] Roizen J, Luedke CE, Herzog ED, Muglia LJ. Oxytocin in the circadian timing of birth. *PLoS One* 2007;2:e922.
- [24] Ochedalski T, Lachowicz A. Maternal and fetal hypothalamo-pituitary-adrenal axis: different response depends upon the mode of parturition. *Neuro Endocrinol Lett* 2004;25:280–4.
- [25] Ratajczak CK, Asada M, Allen GC, McMahon DG, Muglia LM, Smith D, et al. Generation of myometrium-specific *Bmal1* knockout mice for parturition analysis. *Reprod Fertil Dev* 2012; 24:759–67.
- [26] Jin X, Shearman LP, Weaver DR, Zylka MJ, De Vries GJ, Reppert SM. A molecular mechanism regulating rhythmic output from the suprachiasmatic circadian clock. *Cell* 1999;96:57–68.
- [27] Gluckman PD, Hanson MA. Maternal constraint of fetal growth and its consequences. *Semin Fetal Neonatal Med* 2004;9:419–25.
- [28] McLaren A, Renfree MB, Hensleigh HC. Influence of conceptus number and weight on the amount of foetal fluid in the mouse. *J Embryol Exp Morphol* 1976;35:191–6.